Study of alkaloid berberine and its interaction with the human telomeric i-motif DNA structure

R. Gargallo[1]*, A. Aviñó[2], R. Eritja[2], P. Jarosova[3], S. Mazzini[4], L. Scaglioni[4], P. Taborsky[3]*

1. Dept. of Chemical Engineering and Analytical Chemistry, University of Barcelona, Marti i Franquès 1, E-08028 Barcelona, Spain

2. Institute for Advanced Chemistry of Catalonia (IQAC-CSIC), CIBER-BBN, Jordi Girona 18-26, E-08034 Barcelona, Spain

3. Department of Chemistry, Faculty of Science, Masaryk University, Kamenice 5, 62500 Brno, Czech Republic

4. Department of Food, Environmental and Nutritional Sciences (DEFENS), Section of Chemical and Biomolecular Sciences, University of Milan, Via Celoria 2, 20133 Milan, Italy

Abstract

The alkaloid berberine presents many biological activities related to its potential to bind DNA structures, such as duplex or G-quadruplex. Recently, it has been proposed that berberine may interact with i-motif structures formed from the folding of cytosine-rich sequences. In the present work, the interaction of this alkaloid with the i-motif formed by the human telomere cytosine-rich sequence, as well as with several positive and negative controls, has been studied. Molecular fluorescence and circular dichroism spectroscopies, as well as nuclear magnetic resonance spectrometry and competitive dialysis, have been used with this purpose. The results shown here reveal that the interaction of berberine with this i-motif is weak, mostly electrostatics in nature and takes place with bases not involved in $C{\cdot}C^+$ base pairs. Moreover, this ligand is not selective for i-motif structures, as binds equally to both, folded structure, and unfolded strand, without producing any stabilization of the i-motif. As a conclusion, the development of analytical methods based on the interaction of fluorescent ligands, such as berberine, with i-motif structures should consider the thermodynamic aspects related with the interaction, as well as the selectivity of the proposed ligands with different DNA structures, including unfolded strands.

Keywords: berberine, i-motif, DNA binders, G-quadruplex

* To whom correspondence should be addressed

e-mail: raimon_gargallo@ub.edu, phone: +34-934039116

e-mail: taborak@email.cz, phone: +42-0605125644

1. Introduction

DNA may form complex structures apart from the well-known duplex structure firstly proposed by Watson and Crick. Among them, the G-quadruplex and the i-motif structures have gained increased interest because of their *in vitro* properties, but also because of their functions *in vivo* that are still matter of research. G-quadruplex structures are formed by guanine-rich sequences and stabilized by cations, such as potassium or sodium [1]. *In vitro*, G-quadruplex structures have been observed in DNA sequences that may be found at the end of telomeres and near the promoter regions of several oncogenes [2]. On the other hand, the i-motif structures are formed by cytosine-rich sequences usually found at the end of telomeres, centromeres and near the promoter regions of several oncogenes [3]. Structurally, the i-motif consists of two parallel duplexes intercalated in a parallel manner (Figure 1). Duplexes are held together because of the formation of hydrogen bonds between cytosine bases. The protonation of one of the bases at N3 (the pK_a of which is around 4.5) produces the formation of a cytosine·cytosine base pair that is stabilized by three hydrogen bonds. Consequently, the stability of this structure is greatly enhanced at pH values near the pK_a of cytosine, being its stability lower at neutral pH values. The i-motif structure has become a subject of great interest because of its potential role *in vivo* [4], as well as because of applications in other fields, such as Nanotechnology or Analytical Chemistry, among others.

It has been proposed that modulation of the stabilities of G-quadruplex and i-motif structures may be successfully achieved by interaction with appropriate ligands. Among these, natural alkaloids have attracted large attention because of their potential activity against diseases as well as because of their selectivity in front of other DNA structures, such as ubiquitous duplexes [5][6]. The interaction of natural alkaloids with G-quadruplex structures has been studied in detail. As example, the interaction of a few alkaloids with several G-quadruplex structures formed near the promoter regions of *bcl-2*, *c-kit* and *c-myc* oncogenes was studied recently [5]. NMR spectroscopy measurements gave evidence of the location of the chelerythrine alkaloid over both the outer G-quartets in the parallel G-quadruplex structure formed by the Pu22T14T23 sequence, a mutated sequence found near the promoter region of *c-myc* oncogene.

Berberine is a plant alkaloid and together with coptisine, jatrorrhizine, columbamine, corysamine, and palmatine belongs to the group of quaternary protoberberine alkaloids [7]. The protoberberines are distributed in such plant families as *Papaveraceae*, *Berberidaceae* or *Fumariaceae*, among others, as well as a few examples in *Magnoliaceae* and *Convolvulaceae* [8][9]. The molecule of berberine is a planar molecule with an extended π-delocalized system having a partial positive charge on N7 [7] (Figure 1c). It has shown many biological activities, such as antiproliferative [10] [11], antibacterial [12] and antimicrobial [13].

The interaction of berberine with synthetic double-stranded nucleic acids has been studied extensively [14][15]. In general, the results pointed out to an intercalative mode of interaction, with preference for A-T rich sequences, but this is still matter of discussion [16]. Also, the interaction of berberine with G-quadruplex structure has been studied in detail [17][18][19][20]. The results showed that berberine stacks usually on the external G-quartet with a 1:1 (DNA:ligand) stoichiometry and association constant around $1.2 \cdot 10^6$ M^{-1} at 25ºC. Other studies [21] showed that the

interaction of berberine with the G-quadruplex formed by the human telomere sequence did not induce any structural change on it.

On the other hand, the interaction of berberine with i-motif structures has been less studied than the interaction with G-quadruplex structures. Recently, it has been described the interaction of berberine with two sequences found in the ATXN2L and DAP genes, which are particularly very rich in cytosine bases: 5'-$(CCCCCC)_4$-3' and 5'-$(CCCCCG)_4CCCCC$-3' [22]. At pH 7.0, 20°C and in absence of added salt it was observed that this ligand destabilized the folded structures formed by these two sequences with reductions of melting temperature (ΔT_m) around -1.3 and -3.7°C, respectively. Pagano *et al.* have also studied the interaction of berberine with the i-motif structure formed by the sequence 5'-$CCCT(AACCCT)_3$-3', corresponding to the end of the human telomere [23]. The experiments were carried out at pH 4.3 and 5.7 using a 10 mM sodium phosphate buffer and in absence of added salt. In this case, the addition of 5 equivalents of berberine to the DNA sequence did not produce any change of the T_m values at pH 4.3 and 5.7. Measurements based on Nuclear Magnetic Resonance (NMR) and Circular Dichroism (CD) spectroscopies also revealed scarce modification of i-motif structure upon interaction with the ligand. Concomitantly, it has been shown that berberine was not able to induce folding of a cytosine-rich sequence corresponding to the epidermal growth factor receptor (EGFR) oncogene into an i-motif structure [24]. On the other hand, berberine has been proposed as fluorescent ligand that could be used in the design of molecular logic systems based on the fluorescence observed in the presence of i-motif structures [25]. Hence, it seems that severe discrepancies exist among these experimental evidences from fluorescence spectroscopy and previous studies where it was deduced that little or even null interaction occurs.

To our knowledge, there is not any work dealing with the aspects related to the selectivity of the interaction of berberine with i-motif structures. Also, scarce information may be found describing the thermodynamics aspects of the interaction of berberine with i-motif structures, such as association constants or changes in thermodynamic variables related with the thermal stability of the DNA. Finally, little information may be found about structural aspects of the interaction. Hence, the present work was intended initially to characterize the interaction of this ligand with a model i-motif structure found in the human telomeres [26][27]. Several positive and negative control sequences have been used to ascertain the potential interaction of berberine with i-motif structures. In addition to molecular fluorescence, this study has used CD and NMR spectroscopies, as well as competitive dialysis.

The results show the dramatic enhancement of fluorescence of this ligand in presence of DNA. But the increase is not necessarily the result of strong berberine:DNA interaction. Significant changes of berberine fluorescence quantum yield were recorded also in presence of BSA protein [28], lipoproteins [29], cucurbiturils [30] [31], cyclodextrines [32], chlorides [33] and various solvents [34]. Therefore, the increase of fluorescence intensity is rather result of the reduction of dynamic quenching in the presence of DNA or by restriction of intramolecular motion after electrostatic interaction with DNA [35]. Also, the results obtained suggested a non-specific interaction of berberine with any cytosine-rich sequence, independently of the eventual formation of an i-motif structure. Moreover, the study confirms the high affinity of berberine to G-quadruplex suggesting that G-quadruplex binding is a more probable event for the biological activity of this drug than the potential interaction with i-motif.

2. Materials and methods

2.1 Reagents

The DNA sequences (Table 1) were synthesized on an Applied Biosystems 3400 DNA synthesizer using the 1 µM scale synthesis cycle. Standard phosphoramidites were used. Ammonia deprotection was performed overnight at 55°C. The resulting products were purified using Glen-Pak Purification Cartridge (Glen Research, Sterling, VA, USA). The integrity of DNA sequences was checked by means of Mass Spectrometry. DNA strand concentration was determined by absorbance measurements (260 nm) at 90°C using the extinction coefficients calculated using the nearest-neighbour method as implemented on the OligoCalc webpage [36]. Before any experiment, DNA solutions were first heated to 95°C for 20 minutes and then allowed to reach room temperature overnight. KCl, $NaCH_3COO$, CH_3COOH, KH_2PO_4, K_2HPO_4, HCl and LiOH were purchased from Panreac (Castellar del Vallès, Spain). MilliQ® water was used in all experiments. For CD and molecular absorption measurements carried out at pH 5 and 7, acetate and phosphate buffers were used, respectively. The NMR sample of 22nt was prepared as a 0.23 mM solution concentration in H_2O/D_2O (9:1) containing 10 sodium phosphate buffer, pH 5.2. The oligonucleotide samples were heated to 85°C for 1 min and then cooled at room temperature overnight. Stock solutions of drugs were prepared in the same phosphate buffer at 7.4 mM concentration. The solution showed a little of precipitation.

2.2 Instruments and procedures

Fluorescence experiments were monitored using an AB2 Aminco-Bowman spectrofluorimeter. For most of the measurements, excitation wavelength was 348 nm, excitation and emission slits were set to 4 nm, voltage of the photomultiplier was 800 V, and emission was recorded from 480 to 680 nm at 20°C. A Hellma (Jena, Germany) quartz cell (2 x 10-mm path length, and 1500 µl volume) was used. For each measurement, two emission spectra were recorded, averaged, and later smoothed by applying a Savitzky-Golay filter (41 points, third-degree polynomial). For titration of DNA sequences with berberine, a 2 µM DNA solution at the desired pH was titrated with a berberine stock solution prepared in the same buffer conditions. Additional titrations were carried out in the opposite way, i.e., berberine at the desired pH was titrated with several DNA sequences to investigate the ligand binding mechanism [37]. The final DNA:ligand ratio was 1:6.3. For titration of DNA:berberine mixtures (1:3 ratio) with KCl, the initial mixture (2 and 6 µM DNA and ligand, respectively) at the desired pH was titrated with 900 mM KCl solution at the same pH value. The final concentration of KCl was around 150 mM.

Absorbance spectra were recorded on an Agilent 8453 diode array spectrophotometer. The temperature was controlled by means of an 89090A Agilent Peltier device. Hellma quartz cells (10-mm path length, and 1500 or 3000 µl volume) were used. CD spectra were recorded on a Jasco J-810 spectropolarimeter equipped with a temperature control unit. Hellma quartz cells (10 mm path length, 3000 µl volume) were used.

Melting experiments were monitored using either the Agilent-8453 spectrophotometer or the Jasco J-810 spectropolarimeter, both equipped with Peltier units for temperature control. The DNA or DNA:berberine solution was transferred to a covered 10-mm-path-length cell and spectra were recorded at 2°C intervals with a hold time of 3 minutes at each temperature, which yielded an average heating rate of approximately $0.6°C \cdot min^{-1}$. Buffer solutions were 10 mM acetate or phosphate.

The NMR spectra were recorded on a Bruker AV600 spectrometer operating at a frequency of 600.10 MHz, equipped with a 5 mm TXI inverse probe and *z* -axis gradients. The ^{1}H spectra were acquired at variable temperature ranging from 5 to 65°C and were referenced to external DSS (2,2-dimethyl-2-silapentane-5-sulfonate sodium salt) set at 0.00 ppm. Chemical shifts (δ) were measured in ppm. ^{1}H NMR titrations were performed by adding increasing amounts of berberine to the oligonucleotide solution. Several ratios, R=[drug]/[DNA], were considered: R=0, 0.50, 1.0, 2.0, 3.0 and 4.0. Phase sensitive NOESY spectra were acquired at 25°C, in TPPI mode, with 2048 x 1024 complex FIDs. Mixing times ranged from 100 ms to 300 ms. TOCSY spectra were acquired with the use of a MLEV-17 spin-lock pulse (60 ms total duration). All spectra were transformed and weighted with a 90° shifted sine-bell squared function to 4K x 4K real data points.

Competitive dialysis was used to study the selective interaction of berberine with several DNA structures and sequences (see Supplementary Material). A 100 µl volume of 50 mM DNA was dissolved in potassium phosphate buffer (185 mM NaCl, 185 mM KCl, 2 mM NaH_2PO_4, 1 mM Na_2EDTA, 6 mM Na_2HPO_4 at pH 7.0) and introduced into a separated dialysis unit (Slide-A-Lyzert MINI device, 3500MWCO, Thermo Fisher) and a blank sample containing only buffer. All dialysis units could equilibrate during 24 h at room temperature in a beaker containing the 1 µM solution of berberine. At the end of the dialysis experiment, the amount of berberine bound to DNA relative to free berberine in solution was quantified by measuring the fluorescence intensity at 530 nm.

2.3. Data analysis

For the analysis of binding equilibria, fluorescence data obtained along all the titrations of DNA with berberine were fitted to a 1:1 stoichiometry. The analysis is based on that previously used by other authors [38][39]. Briefly, for a 1:1 stoichiometry, such as:

$$DNA + berb \leftrightarrow DNA{:}berb \quad (1)$$

The association constant K_A may be defined:

$$K_A = \frac{[DNA{:}berb]}{[DNA][berb]} \quad (2)$$

The observed fluorescence increase (ΔF) is fitted to the following equation:

$$\Delta F = \left(\frac{\Delta F_{max}}{2C_{DNA}}\right)\left[\{C_{berb} + C_{DNA} + 1/K_A\} - \left\{\sqrt{(C_{berb} + C_{DNA} + 1/K_A)^2 - 4C_{berb}C_{DNA}}\right\}\right] \quad (3)$$

In this equation $\Delta F = F_i - F_0$, being F_i the measured fluorescence after each addition of berberine to DNA, and F_0 the fluorescence intensity of free berberine. Also, C_{DNA} is the analytical (or total) concentration of DNA, and C_{berb} is the analytical concentration of berberine. Both K_A and ΔF_{max} are the parameters to be optimized. Fitting was done by using the "cftool" function as implemented in Matlab R2019®. Goodness of fit was evaluated by calculating the r^2 and the lack-of-fit (%) according to:

$$lack\ of\ fit = 100\sqrt{\frac{\sum(F_i - F_{i,calc})^2}{\sum F_i^2}} \quad (4)$$

In this equation, $F_{i,calc}$ are the calculated fluorescence values according to the optimized K_A and ΔF_{max} values.

For CD or molecular absorption-monitored melting experiments, ellipticity or absorbance data as a function of temperature were analysed as described elsewhere [40] to determine the melting temperatures (T_m), as well as the corresponding changes in enthalpy and entropy. Because of the low DNA concentration used in these experiments and the absence of added electrolyte, these changes may be considered standard changes in enthalpy and entropy (ΔH^o and ΔS^o, respectively). Briefly, the equilibrium may be written as:

$$DNA_{folded} + heat \leftrightarrow DNA_{unfolded} \qquad (5)$$

The equilibrium constant ruling this equilibrium may be written as:

$$K_{unfolding} = \frac{[DNA_{unfolded}]}{[DNA_{folded}]} \qquad (6)$$

For melting experiments, the following expression of the van't Hoff equation may be used to explain the dependence with temperature of both, folded and unfolded forms of DNA:

$$\ln K_{unfolding} = -\frac{\Delta H^o}{RT} + \frac{\Delta S^o}{R} \qquad (7)$$

ΔH^o and ΔS^o are the standard changes in enthalpy and entropy associated to the unfolding of DNA, respectively. $K_{unfolding}$ was calculated from the ellipticity or absorbance traces at a characteristic wavelength, such as ellipticities measured at 263 nm for parallel G-quadruplex or 288 nm for i-motif structures. It was assumed that ΔH^o and ΔS^o do not change throughout the range of temperatures studied here. The used model assumed that DNA unfolding happens through a two-state process, without intermediates. This assumption was checked previously by means of multivariate analysis methods [41]. Alternatively, an estimation of T_m values may be also obtained from the plot of the first derivative of ellipticity or absorbance data as a function of temperature (see Supplementary Material).

3. Results

3.1. Structural information on the DNA sequences

Prior to the study of the interaction of berberine with the DNA sequences considered (Table 1) the formation of folded structures was studied by means of CD spectroscopy and *in silico* simulations. Figure 2 shows the CD spectra measured for all the sequences at pH 7.4 and 5.2 (10 mM sodium phosphate or acetate buffer, 20°C). At pH 7.4, the CD spectrum of T24 shows negative and positive bands of equal magnitude at 250 and 275 nm, respectively, which may be related to a partially stacked single strand [42]. The spectra measured at both pH values are similar, a fact that may be easily explained because of the lack of groups that could be show acid-base properties in this pH range.

The CD spectrum of CT11 at pH 7.4 showed a positive band around 275 nm and a weak negative band around 240 nm. These features have also been assigned to a unfolded single strand [43]. Contrarily to T24, the CD spectrum of CT11 measured at pH 5.2 showed a strong positive band at 285 nm and a negative band at 260 nm, which are clear signatures of the i-motif structure, despite the presence of alternating thymine bases in the sequence [44]. A similar behaviour was observed for 22ntmut, which is a sequence known to form a stable i-motif structure at pH 5.2 [27][45]. The CD spectrum of 20up at pH 7.4 was also like that of T24 at this pH value, which would agree with a partially stacked strand. By using the *mfold* web server [46] (Figure S1) it was possible to predict the formation of both a self-duplex and an internal loop by this sequence at pH 7. Finally, when the pH was lowered to 5.2, only a small reduction of ellipticity was observed. The CD spectrum of 22nt at pH 7.4 was like that of 20up. At this pH value, the predicted folded structures by the *mfold* server were hardly stable. On the other hand, the CD spectrum at pH 5.2 showed clear i-motif signatures, like those observed for 22ntmut. Finally, the CD spectrum of Pu22T14T23 at pH 7.4 was assigned to a parallel G-quadruplex structure [47]. Interestingly, the CD spectrum at pH 5.2 was less intense that at pH 7.4, which could denote the destabilizing effect of the protonation of some adenine bases.

Upon addition of berberine (DNA:berberine 1:5), scarce changes were observed in CD spectra of all sequences at both pH values and only 20up and Pu22T14T23 showed small changes in the UV region of their spectra. Moreover, it was not observed any induced CD band in the visible region that could be related to a relatively strong interaction of the ligand with the DNA [48], as reported previously for other ligands and i-motif-forming sequences [49] or for duplex DNA [50]. Molecular absorption spectra were also measured in the absence and presence of berberine (DNA:berberine 1:5, Figure S2), and compared with the spectrum of 10 μM berberine. The clearest variation of the visible band of berberine was observed in presence of Pu22T14T23 at pH 7.4. Overall, all these observations pointed to the maintenance of the initial structures of DNA in the presence of the drug and a rather weak binding.

3.2. Binding measurements

According to the results obtained, the 22nt sequence folds at 20°C and 100 mM KCl into an i-motif structure at pH 5.2, whereas the unfolded strand may be found at pH 7.4. Firstly, molecular-fluorescence monitored titrations of 22nt sequence with berberine at pH 5.2 (where the i-motif is the major structure) and pH 7.4 (where the unfolded strand is the major species) were done at 20°C and 10 mM acetate or phosphate buffer, respectively (Figure 3). It was observed that fluorescence of berberine was clearly greater at pH 5.2 than at pH 7.4 (roughly 4 times). The

maximum of emission shifted from 542 nm (for free berberine) to 530 nm. This shift can be assigned to the lower polarity of berberine surroundings caused by the vicinity of the oligonucleotide.

From the fluorescence measured at 530 nm along the titration, the association constant was calculated (Table 2). At pH 7.4 and 5.2, the values of the association constants were $4.9 \cdot 10^4$ and $1.1 \cdot 10^5$ M^{-1}, respectively. Hence, it seems that decreasing pH, which favours the formation of the i-motif structure, also produces a stronger interaction between berberine and 22nt. Xu *et al.* determined a dissociation constant (K_D) equal to 19.6 μM for the interaction of a similar sequence, $TA_2(C_3TA_2)_3C_3$, with berberine at pH 6.0 in 10 mM sodium acetate [25]. This value corresponds to an association constant equal to $5.1 \cdot 10^4$ M^{-1}, which is like the values determined here.

To check whether the enhancement of fluorescence at pH 5.2 was related to the formation of i-motif structure or not, similar titrations of positive and negative control sequences were done. With that purpose, Pu22T14T23, T24, CT11, and 20up were titrated with berberine (Figure 4).

The titration of T24 sequence produced a small, rather linear increase in berberine fluorescence at both pH values. From the analysis of data, similar association constants were calculated for both pH values ($3.7 \cdot 10^4$ M^{-1} and $4.7 \cdot 10^4$ M^{-1} at pH 5.2 and 7.4, respectively). This agrees with the absence of acid-base equilibria in this sequence (pK_a of thymine is around 10) [51] and pH-induced conformational changes. The titration of CT11 at pH 7.4, a sequence showing cytosine bases that, which cannot form i-motif structure, showed a similar value of the binding to those determined for T24 at this pH ($4.5 \cdot 10^4$ M^{-1}). However, at pH 5.2, the calculated K_A value is clearly higher ($8.9 \cdot 10^4$ M^{-1}) than that determined at pH 7.4, which could be related with the previously observed folding at this pH (Figure 2). Also, the titration of 20up showed a different behaviour of binding at pH 5.2 ($2 \cdot 10^5$ M^{-1}) in relation to pH 7.4 ($8.5 \cdot 10^4$ M^{-1}).

It is known that in the forward titration of DNA with a ligand, such as those described above, experimental conditions are favourable to the formation of complexes with higher DNA:ligand stoichiometries [37][52]. On the contrary, in the reverse titrations of a ligand with DNA, the ligand concentration is small, being the major species the free DNA, and the next most abundant species the 1:1 complex. To check the consistency of both approaches in the case of the binding of berberine to cytosine-rich sequences, several titrations of berberine with DNA sequences were done. The results obtained (Figure S3) were like those reported in Table 2, which reinforced the hypothesis of a 1:1 stoichiometry for the binding of berberine to cytosine-rich sequences.

Secondly, the interaction of berberine with a G-quadruplex was studied. At the experimental conditions, the G-quadruplex structure folded with a T_m value equal to 41.9°C (Figure S4). Upon addition of berberine to 1:3 ratio, the value of T_m increased to 54.5°C, which indicated a stronger interaction of the ligand with the folded structure than with the unfolded strand. Concomitantly, the standard changes in enthalpy and entropy related to the unfolding of the G-quadruplex were calculated according to equation 7. In both cases, the presence of berberine produced a clear stabilization of the folded structure. Upon addition of the ligand, fluorescence of the berberine:Pu22T14T23 complex increased at both pH values, being the final value slightly greater at pH 7.4 than at pH 5.2 (Figure 4). From the fluorescence measured at 530 nm, association constants were determined (Table 2). At pH 7.4, the value of the association constant agrees quite well with values previously reported for other similar parallel G-quadruplex

structures. Hence, Arora *et al.* [19] reported $\log K_A$ = 6.08 for the binding of berberine with the antiparallel G-quadruplex formed by the telomeric sequence $A(G_3T_2A)G_3$ in the presence of 100 mM KCl, which is similar to the value determined here. The value of the binding constant at pH 5.2 is slightly lower than at pH 7.4, which would agree with the unfolding observed by using CD spectroscopy (Figure 2).

In view of the results shown in Figure 4 and Table 2, it seems that a greater increase of berberine fluorescence in the presence of a given sequence (ΔF_{max}) might not imply a stronger binding (K_A). As example, Figure 5a shows the fluorescence intensity at 530 nm as a function of berberine:22nt ratio (0-10) and temperature (12-30ºC). As T_m of 22nt at pH 5.2 is 53ºC (see below for the melting studies of 22nt), the upper limit of the studied temperature range was set to 30ºC. In this way, it was expected that the i-motif would be the only species present in solution, being residual the presence of unfolded strands. It is well known that fluorescence intensity is generally reduced with increasing temperature due to the greater importance of non-fluorescent decay paths. In the case of the interaction between berberine and 22nt a clear decrease of the fluorescence intensity was observed. However, the calculated association constants are practically equal in this temperature range (Table 2).

From the plot of ln K_A *vs.* 1/T the standard changes in enthalpy and entropy related with this binding were calculated. As the association constant was practically independent on temperature in the range studied, the calculated changes in enthalpy and entropy were low (-0.9 kcal·mol^{-1} and 26.1 cal·K^{-1}·mol^{-1}, respectively). A more accurate application of van't Hoff equation should consider a wider temperature range but, as stated above, this would involve the presence of the unfolded strands, making the results of the calculation not representative. For comparison, the calculated standard changes in enthalpy and entropy values are smaller than those reported for the binding of berberine with single stranded poly(A) [53], where ΔH and ΔS were calculated to be -8.7 kcal·mol^{-1} and 57.5 cal·K^{-1}·mol^{-1}, respectively, in a similar temperature range (15-30ºC) and pH 7.4. On the other hand, the values calculated in the present work are not very different from those reported for the binding of berberine with antiparallel G-quadruplexes at pH 7.4 (ΔH and ΔS equal to -1.2 kcal·mol^{-1} and 21.8 cal·K^{-1}·mol^{-1}, respectively [19] or -2.8 kcal·mol^{-1} and 17.0 cal·K^{-1}·mol^{-1} [21]). According to previous studies by Chaires [54], groove-binding interactions are largely entropically driven, whereas intercalation reactions are driven by large favourable enthalpy contributions and are opposed by entropy. In the present study, the observed low negative change in enthalpy and positive change in entropy have been explained in terms of external stacking rather than intercalation.

At this point, it was clear that the low fluorescence of berberine was enhanced in presence of the folded 22nt at pH 5.2 than in the presence of the unfolded strand at pH 7.4. To characterize the stability of the resulting interaction complex against temperature and pH, CD and NMR spectroscopies were used. The interaction of a folded structure, such as i-motif, with a ligand should produce ideally an increase in its thermal stability, like that observed for Pu22T14T23. CD-monitored melting experiments of 22nt and several 22nt:berberine mixtures were carried out at different pH values to explore this possibility (Figure S5). Within the pH range considered (4.6 – 6.0), the determined T_m values did not show any clear variation due to the presence of the ligand. Also, thermodynamic parameters, such as the standard changes in enthalpy and entropy did not change significantly. This is in contrast to the strong stabilization of the G-quadruplex formed by Pu22T14T23 (ΔT_m ~ 16ºC, Figure S4), in agreement with previous reports on similar alkaloids [5]. All together, these data point to a similar interaction between berberine and both, folded

and unfolded 22nt sequence, i.e., the ligand does not have any preference for the folded i-motif structure over the unfolded strand.

The absence of spectral changes in CD or molecular absorption spectra of the i-motif structure upon addition of berberine suggested the absence of a strong interaction between both molecules. Moreover, the null variation of the melting curve of i-motif in the presence of the ligand suggested a similar interaction with both, folded and unfolded forms of the DNA sequence. Hence, it was deduced that the interaction between berberine and cytosine-rich sequences is mostly electrostatics in nature, ruling out the presence of hydrophobic interactions, such as stacking on nitrogenated bases. To check this hypothesis, a mixture of 22nt:berberine (1:3) was titrated with KCl (Figure 6). It was observed a decrease of fluorescence intensity upon addition of KCl, which was explained as a result of the reduction of the net electric charge on berberine and 22nt upon addition of an inert salt [16]. This reduction produced the weakness of the electrostatic interaction between ligand and DNA. In contrast, addition of KCl to free berberine (Figure S6) produced a weak increase of fluorescence and a concomitant weak decrease of absorbance. This behaviour could be explained because of the reduction of hydrophobic interactions producing stacking of berberine molecules upon addition of KCl.

A similar behaviour was observed along the titration of mixtures of berberine with 20up, T24 and CT11 (Figure 6b). On the other hand, the titration of a mixture of Pu22T14T23:berberine (1:3) showed a smaller reduction of fluorescence upon addition of KCl. This would be in accordance with an interaction model based on hydrophobic (i.e., intercalation or end-stacking) rather than in electrostatic interactions.

It is known that berberine binds strongly to duplex DNA with preference for A·T base pairs [55][56]. The 22nt sequence shows several adenine and thymine bases that could be behind the enhancement of fluorescence upon interaction with the 22nt sequence at pH 5.2. To check this hypothesis, the interaction of berberine with a mutated sequence where all adenine bases were replaced by thymine was also studied (22ntmut, Table 1). It has been shown that these mutations stabilize slightly the i-motif structure formed by 22nt in terms of T_m values ([45] and references therein). First, CD-monitored melting experiments of 22ntmut did not show any shift of T_m value (59.5^{o}C) in presence of the ligand (Figure S7), which pointed again to a mode of interaction similar to that observed for 22nt. Secondly, titrations of 22ntmut with berberine at pH 5.2 showed nearly identical fluorescence increase due to the ligand than in the case of 22nt.

3.3 NMR measurements

To gain insight on the interaction mode, NMR studies were carried out. Spectra of 22nt and 22ntmut oligonucleotides showed sharp peaks at 15-16 ppm region characteristic of i-motif formation (Figure 7). Typically, for i-motif structures, base pairs in the middle of the i-motif core are more stable than those at the flanking ends and near the double-loop region [57]. The ^{1}H spectrum of 22nt shows only three signals between 15 and 16 ppm, and no signals between 12.5-14 ppm, attributable at Watson-Crick base pairs were observed. Moreover, a very broad and weak signals at 11 ppm, attributable at T·T base pair formation, were observed (Figure 7a, R=0). The 22ntmut sequence showed sharp and other less intense signals at 15-16 ppm region, and sharp and broad signals at 11 ppm. This indicates that in solution a major i-motif conformation was present, in a slow exchange, together with a minor i-

motif conformation (Figure 7b, R=0). A lower flexibility in the loop leads to a formation of T·T base pairs that induces a stabilization of the two conformations present in solution.

The titration experiments performed on both sequences revealed that the berberine did not interact strongly with the i-motif structures. No significant chemical shift variations were observed, after the addition of increasing amount of berberine to both oligonucleotides, for signals at 15-16 ppm and the general appearance of the ^{1}H NMR spectra did not change (Figure 7 and Figures S8-S11). However, for the 22nt oligonucleotide, after the addition of berberine, the formation of low intensity signals at 15-16 ppm and the large signal at 11 ppm became a little more intense. Melting experiments monitored with NMR showed no stabilization of the i-motif structure of the 22nt:berberine complex. The melting temperature for the i-motif was found to be 58°C and for the complex at R=4.0 T_m was equal to 57°C, in agreement with CD-monitored melting experiments. For 22ntmut some signals between 15.6 and 15.7 ppm changed after the addition of few amount of berberine (R=0.5). These findings were interpreted because of a small conformational change induced by the berberine in the oligonucleotide. In summary, these results suggest that the interaction of berberine with both sequences was external and weak.

3.4. Competitive dialysis

According to the results presented, the weak electrostatic interaction would produce weak or even null changes in the i-motif structure because of the interaction with the ligand. Also, it implies that the interaction is non-specific and, consequently, any DNA sequence with a base composition like that of the cytosine-rich sequence considered would produce similar fluorescence signal. In this sense, competitive dialysis experiments revealed that berberine has a very low tendency to bind cytosine-rich sequences when exposed to other DNA structures (Figure 8). Hence, high fluorescence signal was observed for those sequences forming G-quadruplex, like DL_40, chair_1, Tel22 and GG1 (see Figure S12 for the detailed sequences). On the contrary, sequences forming i-motif structures, such as 22nt or 24bclc, did not show much more intense signal than that observed for an unfolded strand (T20). Finally, duplex structures (ds6 and Dickerson) also presented low fluorescence intensity. Altogether, these results point out to a high tendency of berberine to bind G-quadruplex structures, whereas little interaction was observed with i-motif structures.

4. Discussion

The study of i-motif structures has gained great interest due to its potential role in Biology, especially since the demonstration of their existence *in vivo* was reported [4], as well as its potential uses in Nanotechnology [58] or as pH sensors [59][60]. Consequently to this interest, there is an active research on the development of i-motif ligands that could modulate their stability in front of pH or temperature changes [61][62]. As example, Abdelhamid *et al.* reported recently the effect of several G-quadruplex ligands on the thermal stability of two sequences extraordinarily rich in cytosines: $(CCCCCC)_4$ (ATXN2L) and $(CCCCCG)_4CCCCC$ (DAP) [22]. These sequences have been shown to fold at neutral pH into i-motif structures. Quite surprisingly, it was observed that many well-known G-quadruplex-stabilizing ligands (BRACO-19, mitoxantrone or pyridostatin) destabilized the i-motif structure at pH 7.0 and 10 mM buffer. In addition, it was also shown that berberine destabilized slightly both folded structures. In a similar way, berberine did not show any stabilizing effect on the i-motif formed by the long sequence

CCCAGCACTGCCCCTCTGGACCCGGTCCCC in 10 mM buffer at pH 5.0 [24]. These works show that the interaction of berberine with i-motif structures seem to be very different from that with G-quadruplex structures, as many works have shown that this ligand is able to stabilize this last structure strongly [63] [64].

Concomitantly, the enhancement of berberine fluorescence by the i-motif formed by the human telomeric sequence at pH 5.0 ($TAA(CCCTAA)_3CCC$) was reported [25]. This observation, which could be considered in disagreement with the practically null effect of the ligand on the i-motif thermal stability, prompted us to study the binding equilibria between berberine and the i-motif structure at acidic pH. Accordingly, spectroscopically monitored binding studies were carried out, not only on the selected i-motif forming sequence but also on a set of sequences able to adopt different spatial structures. At the experimental conditions tested in this work, scarce spectral changes were observed due to the interaction of berberine with the i-motif formed by the chosen sequence. Hence, only fluorescence spectroscopy revealed the existence of an interaction. This is in contrast with the clear CD spectral changes (including the appearance of an induced CD band in the visible region) reported for the interaction of berberine with single stranded poly(A) [53] or poly(G)·poly(C) [65]. In that work, it was also observed that berberine stabilized the structure, a fact that was not observed in the present work.

The behaviour of berberine is similar to that observed for the interaction of other ligands with cytosine-rich sequences, such as fisetin [66] or TMPyP4 [67]. The interaction of this last molecule with an i-motif was confirmed by electrophoretic mobility shift assay, though the melting temperature of the DNA was not altered [67], as observed in the present work. Also, the absence of marked changes of the imino proton signals in ^{1}H-NMR titration experiments suggested that TMPyP4 did not interact with the $C{\cdot}C^+$ base pairs. In fact, the proposed model of interaction showed two porphyrin molecules bound at opposite sides of the i-motif in a symmetrical orientation.

Due to the high sensitivity of the technique, it is possible to observe changes of fluorescence in almost any studied system involving a ligand, such as berberine, and a DNA strand [68]. Even weak interaction with oligonucleotide causes that the berberine molecule is partially shielded by the oligonucleotide. This results in a reduction of collisional quenching of fluorescence by solvent molecules. Therefore, the fluorescence is higher in the presence of all types of oligonucleotides in comparison to free alkaloids. To our knowledge, for the fluorescence intensity is not important if the interaction is weak or strong, it depends rather on the close vicinity of the fluorophore respectively on the polarity of surroundings and accessibility for quenchers [5]. Therefore, the highest increase of fluorescence is usually observed for intercalated molecules into duplex structure [69], followed by probes bonded in grooves and by stacking interactions [5]. The lowest increase is usually observed for weak non-specific electrostatic interaction [70].

Among other causes of reduction of collisional quenching, electrostatic interaction can also cause restriction of vibrational relaxation of berberine molecules. Gu *et al.* [35] suggested that free berberine molecules in aqueous solvent relax part of energy through vibration of methoxy groups and after interaction with DNA can be this non-radiative process significantly reduced. This restriction of molecular motion can result in fluorescence enhancement so called aggregation-induced emission [35].

5. Conclusions

In this work, the interaction of alkaloid berberine with the i-motif DNA structure has been studied by means of spectroscopic methods, focusing on thermodynamic aspects not previously studied. The results have shown that this ligand binds equally to both folded and unfolded cytosine-rich sequences. In conclusion, the development of analytical methods based on the interaction of fluorescent ligands with i-motif structures should consider the thermodynamic aspects related with the interaction, as well as the selectivity of the proposed ligands with different DNA structures, including unfolded strands. Otherwise, the selectivity of the proposed methods could be questioned.

6. Acknowledgments

Oriol Oliva (University of Barcelona, Spain) is thanked for their help in carrying out some of the experiments. Funding from Spanish government (PID2019-107158GB-I00), Italian government (PIANO DI SOSTEGNO ALLA RICERCA 2018 – Linea 2 azione B (DEFENS)) and recognition from the Autonomous Catalan government (2017SGR114) are acknowledged.

7. References

[1] J. Spiegel, S. Adhikari, S. Balasubramanian, The Structure and Function of DNA G-Quadruplexes, Trends Chem. (2019). https://doi.org/10.1016/J.TRECHM.2019.07.002.

[2] S. Neidle, Quadruplex Nucleic Acids as Novel Therapeutic Targets, J. Med. Chem. 59 (2016) 5987–6011. https://doi.org/10.1021/acs.jmedchem.5b01835.

[3] H. Abou Assi, M. Garavís, C. González, M.J. Damha, i-Motif DNA: structural features and significance to cell biology, Nucleic Acids Res. (2018) 1–19. https://doi.org/10.1093/nar/gky735.

[4] M. Zeraati, D.B. Langley, P. Schofield, A.L. Moye, R. Rouet, W.E. Hughes, T.M. Bryan, M.E. Dinger, D. Christ, I-motif DNA structures are formed in the nuclei of human cells, Nat. Chem. 10 (2018) 631–637. https://doi.org/10.1038/s41557-018-0046-3.

[5] P. Jarošová, P. Paroulek, M. Rajecky, V. Rajecka, E. Taborska, R. Eritja, A. Aviñó, S. Mazzini, R. Gargallo, P. Táborský, Naturally occurring quaternary benzo[: C] phenanthridine alkaloids selectively stabilize G-quadruplexes, Phys. Chem. Chem. Phys. 20 (2018) 21772–21782. https://doi.org/10.1039/c8cp02681e.

[6] P. Jarošová, R. Sándor, A. Slaninková, M. Vido, O. Peš, P. Táborský, Quaternary protoberberine alkaloids and their interactions with DNA, Chem. Pap. 73 (2019) 2965–2973. https://doi.org/10.1007/s11696-019-00857-z.

[7] L. Grycova, J. Dostal, R. Marek, Quaternary protoberberine alkaloids, Phytochemistry. 68 (2007) 150–175.

[8] K.W. Bentley, β-Phenylethylamines and the isoquinoline alkaloids, Nat. Prod. Rep. 23 (2006) 444–463. https://doi-org.sire.ub.edu/10.1039/B509523A.

[9] K. Šebrlová, O. Peš, I. Slaninová, O. Vymazal, J. Kantorová, E. Táborská, Seasonal variation in alkaloid composition and antiproliferative activity of Stylophorum lasiocarpum (Oliv.) Fedde, Chem. Pap. 69 (2015) 698–708. https://doi.org/10.1515/chempap-2015-0083.

[10] I. Slaninová, E. Táborská, H. Bochořáková, J. Slanina, Interaction of benzo[c]phenanthridine and protoberberine alkaloids with animal and yeast cells, Cell Biol. Toxicol. 17 (2001) 51–63. https://doi.org/10.1023/A:1010907231602.

[11] K. Wang, X. Feng, L. Chai, S. Cao, F. Qiu, The metabolism of berberine and its contribution to the pharmacological effects, Drug Metab. Rev. 49 (2017) 139–157. https://doi.org/10.1080/03602532.2017.1306544.

[12] M.S. Hossan, H. Jindal, S. Maisha, C. Samudi Raju, S. Devi Sekaran, V. Nissapatorn, F. Kaharudin, L. Su Yi, T.J. Khoo, M. Rahmatullah, C. Wiart, Antibacterial effects of 18 medicinal plants used by the Khyang tribe in Bangladesh, Pharm. Biol. 56 (2018) 201–208. https://doi.org/10.1080/13880209.2018.1446030.

[13] H.-H. Yu, K.-J. Kim, J.-D. Cha, H.-K. Kim, Y.-E. Lee, N.-Y. Choi, Y.-O. You, Antimicrobial Activity of Berberine Alone and in Combination with Ampicillin or Oxacillin Against Methicillin-Resistant Staphylococcus aureus, J. Med. Food. 8 (2005) 454–461. https://doi.org/10.1089/jmf.2005.8.454.

[14] K. Bhadra, G.S. Kumar, Therapeutic Potential of NucleicAcid-Binding Isoquinoline Alkaloids: Binding Aspects and Implications forDrug Design, Med. Res. Rev. 31 (2011) 821–862. https://doi.org/10.1002/med.

[15] D. Bhowmik, G. Suresh Kumar, Recent Advances in Nucleic Acid Binding Aspects of Berberine Analogs and Implications for Drug Design, Mini-Reviews Med. Chem. 16 (2015) 104–119. https://doi.org/10.2174/1389557515666150909144425.

[16] N. Kundu, A. Roy, D. Banik, N. Sarkar, Unveiling the Mode of Interaction of Berberine Alkaloid in Different Supramolecular Confined Environments: Interplay of Surface Charge between Nano-Confined Charged Layer and DNA, J. Phys. Chem. B. 120 (2016) 1106–1120. https://doi.org/10.1021/acs.jpcb.5b10121.

[17] W.J. Zhang, T.M. Ou, Y.J. Lu, Y.Y. Huang, W. Bin Wu, Z.S. Huang, J.L. Zhou, K.Y. Wong, L.Q. Gu, 9-Substituted berberine derivatives as G-quadruplex stabilizing ligands in telomeric DNA, Bioorganic Med. Chem. 15 (2007) 5493–5501. https://doi.org/10.1016/j.bmc.2007.05.050.

[18] M. Franceschin, L. Rossetti, A. D'Ambrosio, S. Schirripa, A. Bianco, G. Ortaggi, M. Savino, C. Schultes, S. Neidle, Natural and synthetic G-quadruplex interactive berberine derivatives, Bioorganic Med. Chem. Lett. 16 (2006) 1707–1711. https://doi.org/10.1016/j.bmcl.2005.12.001.

[19] A. Arora, C. Balasubramanian, N. Kumar, S. Agrawal, R.P. Ojha, S. Maiti, Binding of berberine to human telomeric quadruplex - Spectroscopic, calorimetric and molecular modeling studies, FEBS J. 275 (2008) 3971–3983. https://doi.org/10.1111/j.1742-4658.2008.06541.x.

[20] C. Shan, J.H. Tan, T.M. Ou, Z.S. Huang, Natural products and their derivatives as G-quadruplex binding ligands, Sci. China Chem. 56 (2013) 1351–1363. https://doi.org/10.1007/s11426-013-4920-y.

[21] D. Bhowmik, G. Fiorillo, P. Lombardi, G. Suresh Kumar, Recognition of human telomeric G-quadruplex DNA by berberine analogs: Effect of substitution at the 9 and 13 positions of the isoquinoline moiety, J. Mol. Recognit. 28 (2015) 722–730. https://doi.org/10.1002/jmr.2486.

[22] M.A.S. Abdelhamid, A.J. Gates, Z.A.E. Waller, Destabilization of i-Motif DNA at Neutral pH by G-Quadruplex Ligands, Biochemistry. 58 (2019) 245–249. https://doi.org/10.1021/acs.biochem.8b00968.

[23] A. Pagano, N. Iaccarino, M.A.S. Abdelhamid, D. Brancaccio, E.U. Garzarella, A. Di Porzio, E. Novellino, Z.A.E. Waller, B. Pagano, J. Amato, A. Randazzo, Common G-quadruplex binding agents found to interact with i-motif-forming DNA: Unexpected multi-target-directed compounds, Front. Chem. 6 (2018) 1–13. https://doi.org/10.3389/fchem.2018.00281.

[24] C. Sissi, C. Cristofari, M. Ghezzo, R. Rigo, M.L. Greco, pH-driven conformational switch between non-canonical DNA structures in a C-rich domain of EGFR promoter, Sci. Rep. 9 (2019) 1–11. https://doi.org/10.1038/s41598-018-37968-8.

[25] L. Xu, S. Hong, N. Sun, K. Wang, L. Zhou, L. Ji, R. Pei, Berberine as a novel light-up i-motif fluorescence ligand and its application in designing molecular logic systems, Chem. Commun. 52 (2016) 179–182. https://doi.org/10.1039/c5cc08242k.

[26] S. Pérez-Rentero, R. Gargallo, C. González, R. Eritja, Modulation of the stability of i-motif structures using an acyclic threoninol cytidine derivative, RSC Adv. 5 (2015) 63278–63281. https://doi.org/10.1039/c5ra10096h.

[27] S. Fernández, R. Eritja, A. Aviñó, J. Jaumot, R. Gargallo, Influence of pH, temperature and the cationic porphyrin TMPyP4 on the stability of the i-motif formed by the 5'-(C3TA2)4-3' sequence of the human telomere, Int. J. Biol. Macromol. 49 (2011) 729–736. https://doi.org/10.1016/j.ijbiomac.2011.07.004.

[28] Y.-J. Hu, Y. Ou-Yang, C.-M. Dai, Y. Liu, X.-H. Xiao, Binding of berberine to bovine serum albumin: spectroscopic approach, Mol. Biol. Rep. 37 (2010) 3827–3832. https://doi.org/10.1007/s11033-010-0038-x.

[29] N.L. Andreazza, C. Vevert-Bizet, G. Bourg-Heckly, F. Sureau, M. José Salvador, S. Bonneau, Berberine as a photosensitizing agent for antitumoral photodynamic therapy: Insights into its association to low density lipoproteins, Int. J. Pharm. 510 (2016) 240–249. https://doi.org/https://doi.org/10.1016/j.ijpharm.2016.06.009.

[30] Z. Miskolczy, L. Biczók, Kinetics and Thermodynamics of Berberine Inclusion in Cucurbit[7]uril, J. Phys. Chem. B. 118 (2014) 2499–2505. https://doi.org/10.1021/jp500603g.

[31] Y.P. Li, H. Wu, L.M. Du, Study on the inclusion interactions of berberine hydrochloride and cucurbit[7] by spectrofluorimetry, Chinese Chem. Lett. 20 (2009) 322–325. https://doi.org/https://doi.org/10.1016/j.cclet.2008.10.045.

[32] B. Jia, Y. Li, D. Wang, R. Duan, Study on the Interaction of β-Cyclodextrin and Berberine Hydrochloride and Its Analytical Application, PLoS One. 9 (2014) e95498. https://doi.org/10.1371/journal.pone.0095498.

[33] M. Megyesi, L. Biczók, Effect of ion pairing on the fluorescence of berberine, a natural isoquinoline alkaloid, Chem. Phys. Lett. 447 (2007) 247–251. https://doi.org/https://doi.org/10.1016/j.cplett.2007.09.046.

[34] M.S. Díaz, M.L. Freile, M.I. Gutiérrez, Solvent effect on the UV/Vis absorption and fluorescence spectroscopic properties of berberine, Photochem. Photobiol. Sci. 8 (2009) 970–974. https://doi.org/10.1039/B822363G.

[35] Y. Gu, Z. Zhao, H. Su, P. Zhang, J. Liu, G. Niu, S. Li, Z. Wang, R.T.K.K. Kwok, X.-L.L. Ni, J. Sun, A. Qin, J.W.W.Y.Y. Lam, B.Z. Tang, Exploration of biocompatible AIEgens from natural resources, Chem. Sci. 9 (2018) 6497–6502. https://doi.org/10.1039/c8sc01635f.

[36] W.A. Kibbe, Oligo Calc: an online oligonucleotides properties calculator, Nucleic Acids Res. 35 (2007) W43–W46. https://doi.org/10.1093/nar/gkm234.

[37] V. Gabelica, R. Maeda, T. Fujimoto, H. Yaku, T. Murashima, N. Sugimoto, D. Miyoshi, Multiple and Cooperative Binding of Fluorescence Light-up Probe Thioflavin T with Human Telomere DNA G-Quadruplex, Biochemistry. 52 (2013) 5620–5628. https://doi.org/10.1021/bi4006072.

[38] S. Maiti, N.K. Chaudhury, S. Chowdhury, Hoechst 33258 binds to G-quadruplex in the promoter region of human c-myc, Biochem. Biophys. Res. Commun. 310 (2003) 505–512. https://doi.org/10.1016/j.bbrc.2003.09.052.

[39] P. Thordarson, Determining association constants from titration experiments in supramolecular chemistry, Chem. Soc. Rev. 40 (2011) 1305–1323. https://doi.org/10.1039/C0CS00062K.

[40] J.D. Puglisi, I.B.T.-M. in E. Tinoco, [22] absorbance melting curves of RNA, in: RNA Process. Part A Gen. Methods, Academic Press, 1989: pp. 304–325. https://doi.org/https://doi.org/10.1016/0076-6879(89)80108-9.

[41] R. Gargallo, Hard/Soft hybrid modeling of temperature-induced unfolding processes involving G-quadruplex and i-motif nucleic acid structures, Anal. Biochem. 466 (2014) 4–15. https://doi.org/10.1016/j.ab.2014.08.008.

[42] N.L. Goddard, G. Bonnet, O. Krichevsky, A. Libchaber, Sequence Dependent Rigidity of Single Stranded DNA, Phys. Rev. Lett. 85 (2000) 2400–2403. https://doi.org/10.1103/PhysRevLett.85.2400.

[43] J. Kypr, I. Kejnovská, D. Renčiuk, M. Vorlíčková, Circular dichroism and conformational polymorphism of DNA, Nucleic Acids Res. 37 (2009) 1713–1725. https://doi.org/10.1093/nar/gkp026.

[44] P. Školáková, D. Renčiuk, J. Palacký, D. Krafčík, Z. Dvořáková, I. Kejnovská, K. Bednářová, M. Vorlíčková, Systematic investigation of sequence requirements for DNA i-motif formation, Nucleic Acids Res. 47 (2019) 2177–2189. https://doi.org/10.1093/nar/gkz046.

[45] S. Benabou, M. Garavís, S. Lyonnais, R. Eritja, C. González, R. Gargallo, Understanding the effect of the nature of the nucleobase in the loops on the stability of the i-motif structure, Phys. Chem. Chem. Phys. 18 (2016) 7997–8004. https://doi.org/10.1039/c5cp07428b.

[46] M. Zuker, Mfold web server for nucleic acid folding and hybridization prediction, Nucleic Acids Res. 31 (2003) 3406–3415. https://doi.org/10.1093/nar/gkg595.

[47] S. Mazzini, R. Gargallo, L. Musso, F. De Santis, A. Aviñó, L. Scaglioni, R. Eritja, M. Di Nicola, F. Zunino, A. Amatulli, S. Dallavalle, Stabilization of c-KIT G-Quadruplex DNA Structures by the RNA Polymerase I Inhibitors BMH-21 and BA-41, Int. J. Mol. Sci. 20 (2019) 4927. https://doi.org/10.3390/ijms20194927.

[48] E.W. White, F. Tanious, M.A. Ismail, A.P. Reszka, S. Neidle, D.W. Boykin, W.D. Wilson, Structure-specific recognition of quadruplex DNA by organic cations: Influence of shape, substituents and charge, Biophys. Chem. 126 (2007) 140–153. https://doi.org/10.1016/j.bpc.2006.06.006.

[49] N. Khan, A. Aviñó, R. Tauler, C. González, R. Eritja, R. Gargallo, Solution equilibria of the i-motif-forming region upstream of the B-cell lymphoma-2 P1 promoter, Biochimie. 89 (2007) 1562–1572. https://doi.org/10.1016/j.biochi.2007.07.026.

[50] M. Vives, R. Gargallo, R. Tauler, Study of the intercalation equilibrium between the polynucleotide poly(adenylic)-poly(uridylic) acid and the ethidium bromide dye by means of multivariate curve resolution and the multivariate extension of the continuous variation and mole ratio methods, Anal. Chem. 71 (1999) 4328–4337. https://doi.org/10.1021/ac990131m.

[51] V.A. Bloomfield, D.M. Crothers, Ignacio Tinoco, Nucleic Acids. Structures, properties and functions, University Science Books, Sausalito, CA, USA, 1999.

[52] I. Buchholz, B. Karg, J. Dickerhoff, A. Sievers-Engler, M. Lämmerhofer, K. Weisz, Selective Targeting of G-Quadruplex Structures by a Benzothiazole-Based Binding Motif, Chem. – A Eur. J. 23 (2017) 5814–5823. https://doi.org/10.1002/chem.201700298.

[53] R.C. Yadav, G.S. Kumar, K. Bhadra, P. Giri, R. Sinha, S. Pal, M. Maiti, Berberine, a strong polyriboadenylic acid binding plant alkaloid: Spectroscopic, viscometric, and thermodynamic study, Bioorganic Med. Chem. 13 (2005) 165–174. https://doi.org/10.1016/j.bmc.2004.09.045.

[54] J.B. Chaires, A thermodynamic signature for drug-DNA binding mode, Arch. Biochem. Biophys. 453 (2006) 26–31. https://doi.org/10.1016/j.abb.2006.03.027.

[55] S. Chatterjee, S. Mallick, F. Buzzetti, G. Fiorillo, T.M. Syeda, P. Lombardi, K. Das Saha, G.S. Kumar, New 13-pyridinealkyl berberine analogues intercalate to DNA and induce apoptosis in HepG2 and MCF-7 cells through ROS mediated p53 dependent pathway: Biophysical, biochemical and molecular modeling studies, RSC Adv. 5 (2015) 90632–90644. https://doi.org/10.1039/c5ra17214d.

[56] X.-L. Li, Y.-J. Hu, H. Wang, B.-Q. Yu, H.-L. Yue, Molecular Spectroscopy Evidence of Berberine Binding to DNA: Comparative Binding and Thermodynamic Profile of Intercalation, Biomacromolecules. 13 (2012) 873–880. https://doi.org/10.1021/bm2017959.

[57] A.L. Lieblein, B. Fürtig, H. Schwalbe, Optimizing the Kinetics and Thermodynamics of DNA i-Motif Folding, ChemBioChem. 14 (2013) 1226–1230. https://doi.org/10.1002/cbic.201300284.

[58] J. Dash, M. Debnath, K. Fatma, Chemical Regulation of DNA i-Motifs for Nanobiotechnology and Therapeutics, Angew. Chemie Int. Ed. (2019). https://doi.org/10.1002/anie.201813288.

[59] A. Dembska, P. Bielecka, B. Juskowiak, pH-Sensing fluorescence oligonucleotide probes based on an i-motif scaffold: A review, Anal. Methods. 9 (2017) 6092–6106. https://doi.org/10.1039/c7ay01942d.

[60] J.J. Alba, A. Sadurní, R. Gargallo, Nucleic Acid i-Motif Structures in Analytical Chemistry, Crit. Rev. Anal. Chem. 46 (2016) 443–454. https://doi.org/10.1080/10408347.2016.1143347.

[61] S.S. Masoud, K. Nagasawa, i-Motif-Binding Ligands and Their Effects on the Structure and Biological Functions of i-Motif, Chem. Pharm. Bull. 66 (2018) 1091–1103. https://doi.org/10.1248/cpb.c18-00720.

[62] J. Amato, N. Iaccarino, A. Randazzo, E. Novellino, B. Pagano, Noncanonical DNA secondary structures as drug targets: The prospect of the i-motif, ChemMedChem. 9 (2014) 2026–2030. https://doi.org/10.1002/cmdc.201402153.

[63] I. Bessi, C. Bazzicalupi, C. Richter, H.R.A. Jonker, K. Saxena, C. Sissi, M. Chioccioli, S. Bianco, A.R. Bilia, H. Schwalbe, P. Gratteri, Spectroscopic, molecular modeling, and NMR-spectroscopic investigation of the binding mode of the natural alkaloids berberine and sanguinarine to human telomeric G-quadruplex DNA, ACS Chem. Biol. 7 (2012) 1109–1119. https://doi.org/10.1021/cb300096g.

[64] X. Cui, S. Lin, G. Yuan, Spectroscopic probing of recognition of the G-quadruplex in c-kit promoter by small-molecule natural products, Int. J. Biol. Macromol. 50 (2012) 996–1001. https://doi.org/10.1016/j.ijbiomac.2012.02.029.

[65] G.S. Kumar, S. Das, K. Bhadra, M. Maiti, Protonated forms of poly[d(G-C)] and poly(dG).poly(dC) and Their interaction with berberine, Bioorg. Med. Chem. 11 (2003) 4861–4870. https://doi.org/https://doi.org/10.1016/j.bmc.2003.09.028.

[66] S. Takahashi, S. Bhattacharjee, S. Ghosh, N. Sugimoto, S. Bhowmik, Preferential targeting cancer-related i-motif DNAs by the plant flavonol fisetin for theranostics applications, Sci. Rep. 10 (2020) 1–13. https://doi.org/10.1038/s41598-020-59343-2.

[67] O.Y. Fedoroff, A. Rangan, V. V. Chemeris, L.H. Hurley, Cationic porphyrins promote the formation of i-motif DNA and bind peripherally by a nonintercalative mechanism, Biochemistry. 39 (2000) 15083–15090. https://doi.org/10.1021/bi001528j.

[68] D. Suh, J.B. Chaires, Criteria for the mode of binding of DNA binding agents, Bioorganic Med. Chem. 3 (1995) 723–728. https://doi.org/10.1016/0968-0896(95)00053-J.

[69] J. Li, B. Li, Y. Wu, S. Shuang, C. Dong, M.M.F. Choi, Luminescence and binding properties of two isoquinoline alkaloids chelerythrine and sanguinarine with ctDNA, Spectrochim. Acta Part A Mol. Biomol. Spectrosc. 95 (2012) 80–85. https://doi.org/https://doi.org/10.1016/j.saa.2012.04.075.

[70] L.-P. Bai, Z.-Z. Zhao, Z. Cai, Z.-H. Jiang, DNA-binding affinities and sequence selectivity of quaternary benzophenanthridine alkaloids sanguinarine, chelerythrine, and nitidine, Bioorg. Med. Chem. 14 (2006) 5439–5445. https://doi.org/https://doi.org/10.1016/j.bmc.2006.05.012.

[71] A.T. Phan, M. Guéron, J.-L. Leroy, The solution structure and internal motions of a fragment of the cytidine-rich strand of the human telomere, J. Mol. Biol. 299 (2000) 123–144. https://doi.org/10.1006/jmbi.2000.3613.

8. Tables

DNA	Sequence (5' → 3')	Expected major structure in 10 mM buffer and 20°C
22nt	CCC TAA CCC TAA CCC TAA CCC T	i-motif at pH 5.2 / unfolded at pH 7.4
22ntmutT	CCC TTT CCC TTT CCC TTT CCC T	i-motif at pH 5.2 / unfolded at pH 7.4
Pu22T14T23	TGA GGG TGG GTA GGG TGG GTA A	Parallel G-quadruplex at pH 5.2 and 7.4
T24	TTT TTT TTT TTT TTT TTT TTT TTT	Unfolded
20up	CTC GAT GAC TCA ATG ACT CG	Unfolded
CT11	CTC TCT CTC TCT CTC TCT CTC T	Unfolded

Table 1. DNA sequences studied in this work.

pH 5.2	T(°C)	K_A (10^5 M^{-1})	ΔF_{max}	r^2	lack of fit (%)
22nt	12	1.17±0.08	91.7±2.1	0.9997	0.65
22nt	20	1.12±0.29	67.6±2.3	0.9998	0.99
22nt	30	1.07±0.13	37.5±3.0	0.9979	1.95
T24	20	3.72±0.86	59.0±9.8	0.9985	1.83
CT11	20	0.89±0.10	58.4±3.9	0.9986	1.78
20up	20	2.00±0.24	31.8±1.5	0.9990	1.32
Pu22T14T23	20	4.37±0.64	66.6±3.4	0.9969	2.13
pH 7.4	**T(°C)**	**K_A (10^5 M^{-1})**	**ΔF_{max}**	**r^2**	**lack of fit (%)**
22nt	20	0.49±0.23	24.7±8.3	0.9920	2.12
T24	20	0.48±0.15	37.1±8.1	0.9969	2.61
CT11	20	0.45±0.07	21.0±2.4	0.9985	1.81
20up	20	0.85±0.10	41.6±3.4	0.9990	1.44
Pu22T14T23	20	9.12±0.26	72.5±3.8	0.9933	2.94

Table 2. Values of the association constant K_A and ΔF_{max}, as well as their corresponding uncertainties (95 % confidence level) and fitting parameters, calculated for the interaction between berberine and the selected DNA sequences. The equations shown in “Materials and Methods” were applied.

9. Figure captions

Figure 1. (a) Cytosine-protonated cytosine base pair. (b) NMR structure of an intramolecular model i-motif structure formed by the C3TA25mCC2TA2C3UA2C3T sequence (PDB code 1EL2, [71]). This structure, despite not being studied in this work, may be considered as a general example of intramolecular folding. The i-motif structure was generated by using the Molecule Viewer toolbox as implemented in Matlab(R). (c) Berberine.

Figure 2. CD spectra of 2 μM DNAs (blue) and 1:5 (2 μM DNA : 10 μM berberine) mixtures (orange) at pH 7.4 and 5.2. Other conditions were 10 mM sodium phosphate or acetate buffer, 20°C.

Figure 3. Fluorescence spectra measured along the titration of 22nt with berberine at pH 5.2 (a) and 7.4 (b). Insets show the calculated (red line) *vs.* experimental (blue symbols) fluorescence intensities at 530 nm. Experimental conditions were 10 mM sodium acetate or phosphate buffer, 20°C.

Figure 4. Fluorescence measured at 530 nm along the titration of DNA sequences with berberine at pH 5.2 (a) and 7.4 (b). Experimental conditions were 20°C and 10 mM acetate or phosphate buffer, respectively.

Figure 5. Dependence of fluorescence intensity of several 22nt:berberine mixtures with temperature (a) and dependence of the determined association constant with temperature (b). Experimental conditions were 10 mM acetate buffer.

Figure 6. (a) Fluorescence emission spectra measured along the titration of a 22nt:berberine mixture (1:3) at pH 5.2 with KCl. Experimental conditions were 2 μM 22nt, 6 μM berberine, 10 mM sodium acetate, 20°C. (b) Fluorescence emission at 530 nm *vs.* KCl concentration for several sequences in 10 mM sodium acetate, 20°C. Titration involving Pu22T14T23 was carried out at pH 7.4.

Figure 7. ^{1}H NMR spectra of the complexes 22nt (a) and 22ntmut (b) with berberine at different ratios (R). 10 mM sodium phosphate buffer in H_2O/D_2O (9:1), pH 5.2, T=25°C.

Figure 8. Competitive dialysis experiment of berberine against different DNA structures. The sequences used in this experiment are given as Figure S12.

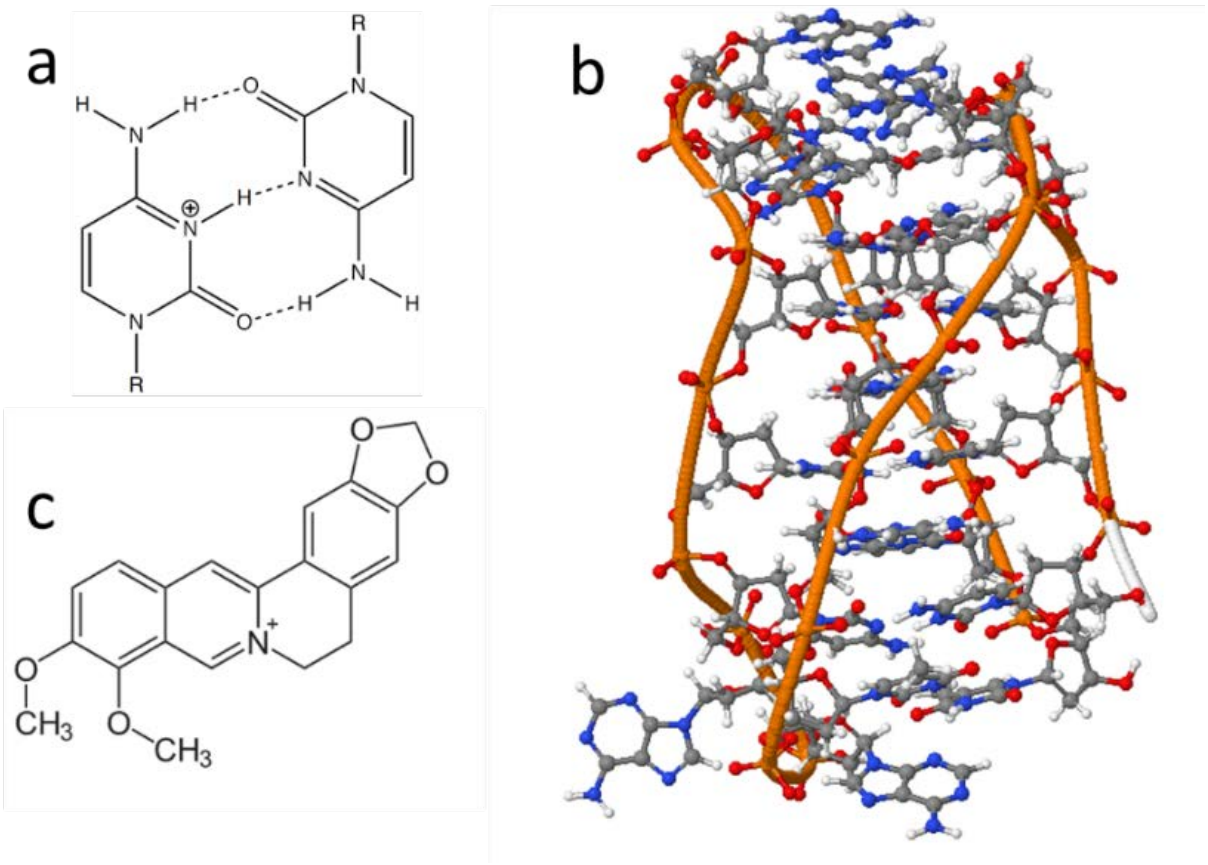

Figure 1.

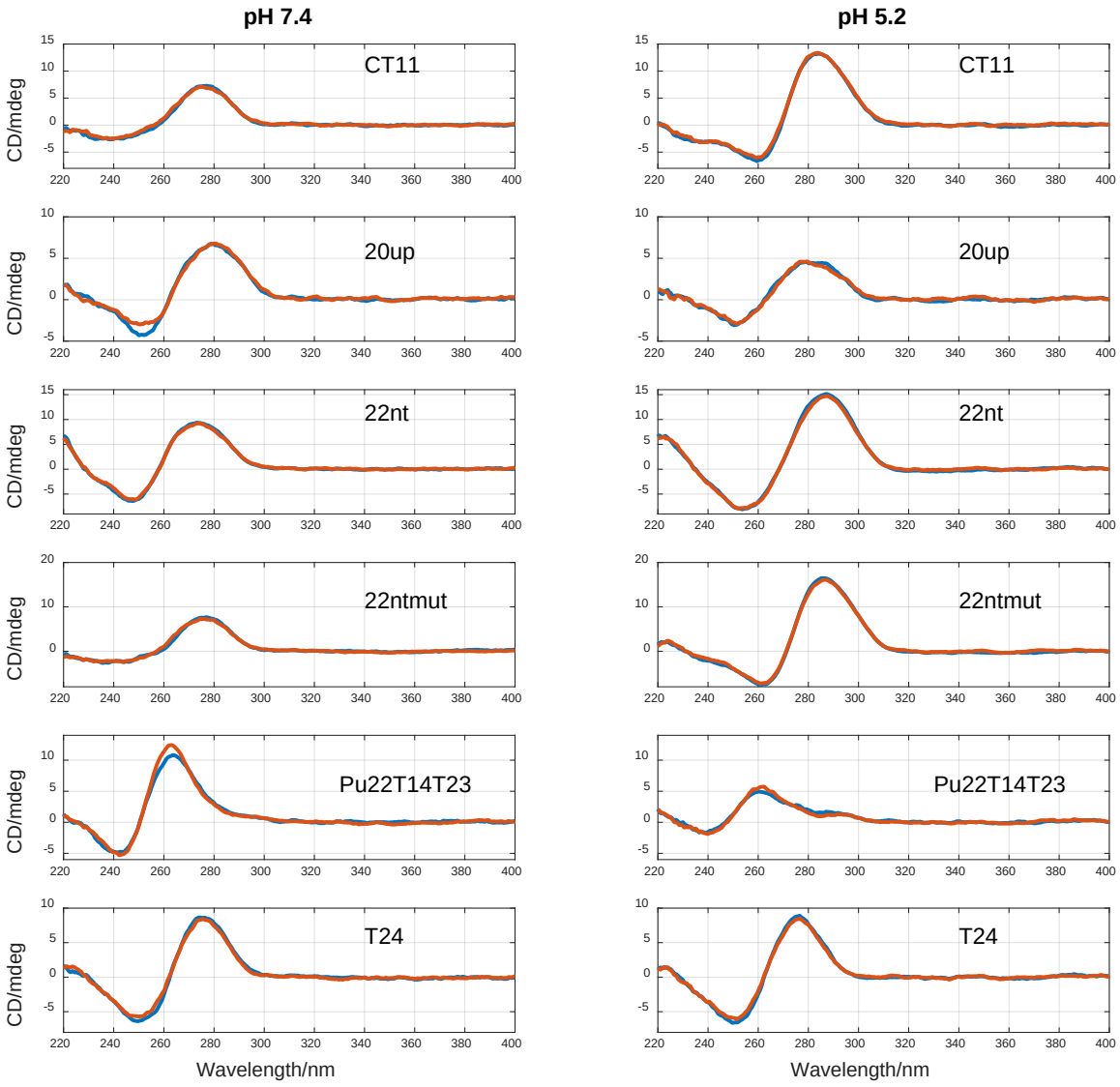
pH 7.4
pH 5.2
CT11
20up
22nt
22ntmut
Pu22T14T23
T24
CD/mdeg
Wavelength/nm

Figure 2

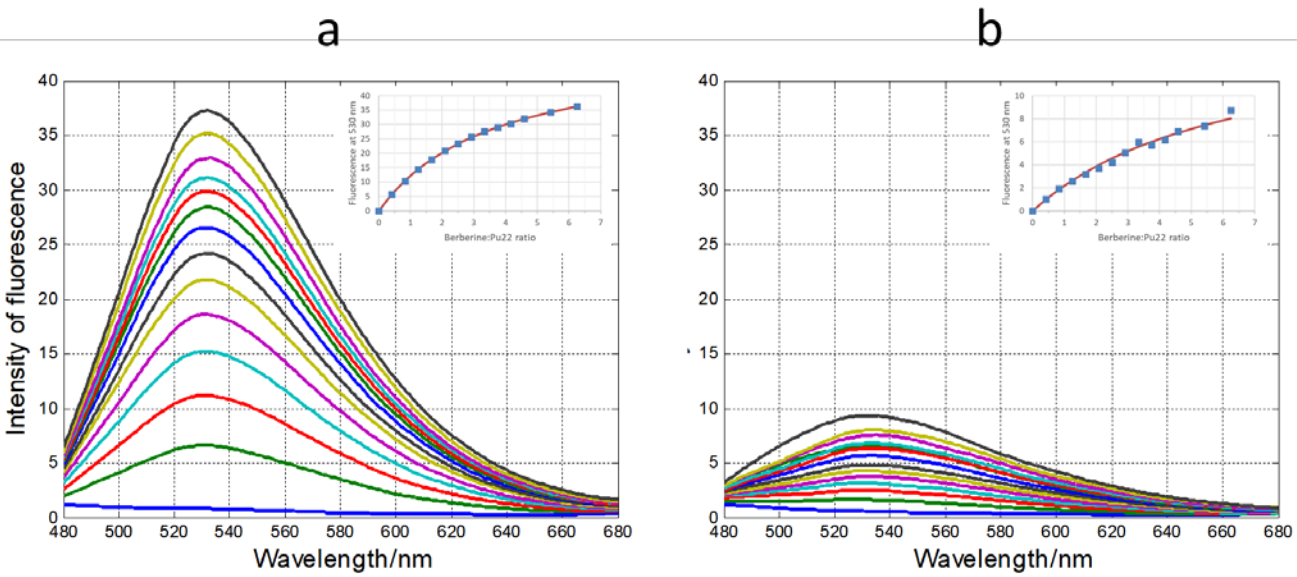
a
b
Intensity of fluorescence
Wavelength/nm
Wavelength/nm
Fluorescence at 530 nm
Berberine:Pu22 ratio
Fluorescence at 530 nm
Berberine:Pu22 ratio

Figure 3.

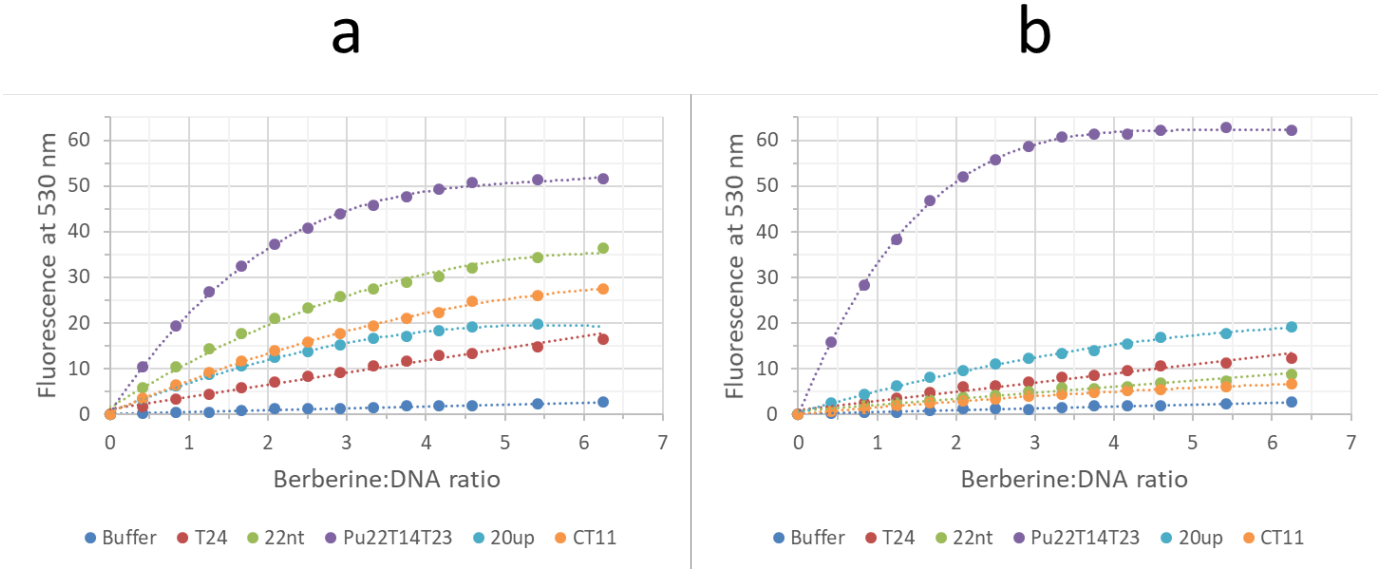
a
b
Fluorescence at 530 nm
Berberine:DNA ratio
Buffer
T24
22nt
Pu22T14T23
20up
CT11

Figure 4.

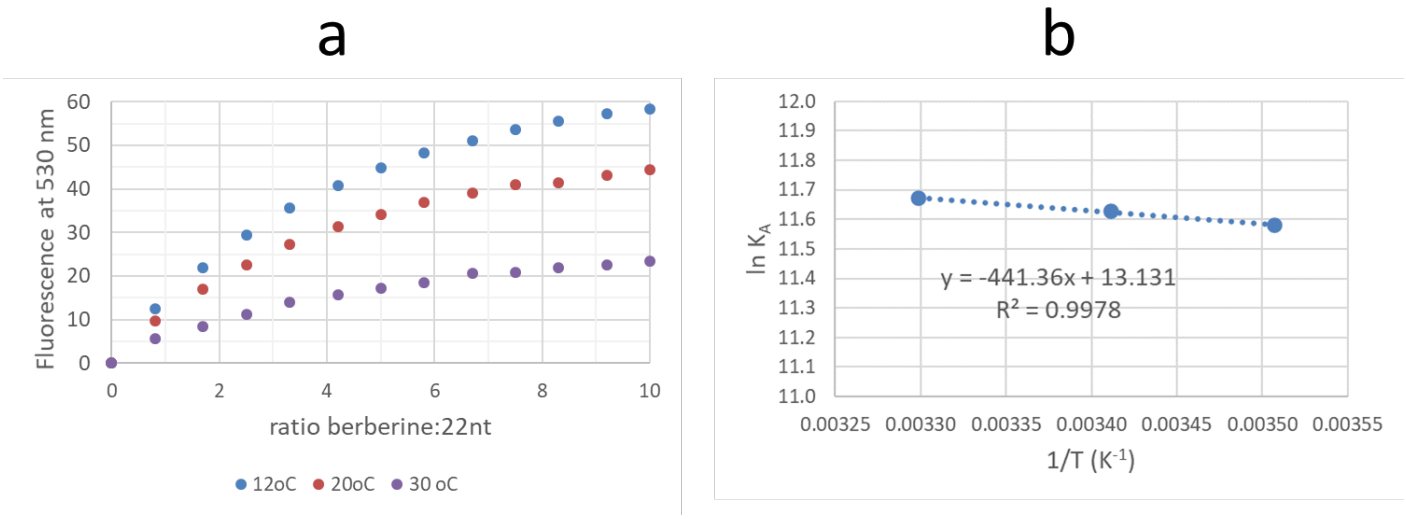
a
b
Fluorescence at 530 nm
ratio berberine:22nt
12oC
20oC
30 oC
ln K_A
y = -441.36x + 13.131
R² = 0.9978
1/T (K⁻¹)

Figure 5.

a

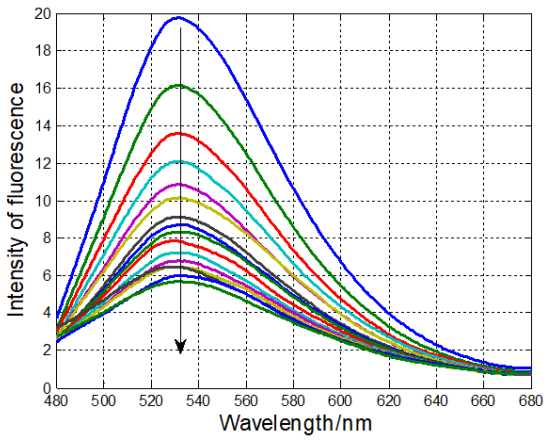
Intensity of fluorescence
Wavelength/nm
0
2
4
6
8
10
12
14
16
18
20
480
500
520
540
560
580
600
620
640
660
680

b

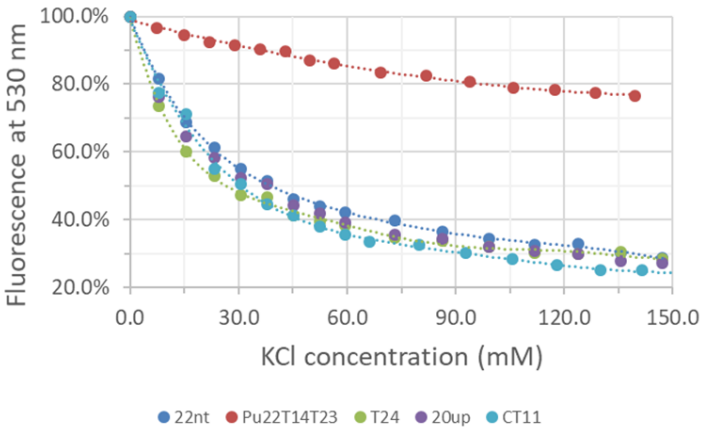
Fluorescence at 530 nm
100.0%
80.0%
60.0%
40.0%
20.0%
0.0
30.0
60.0
90.0
120.0
150.0
KCl concentration (mM)
22nt
Pu22T14T23
T24
20up
CT11

Figure 6.

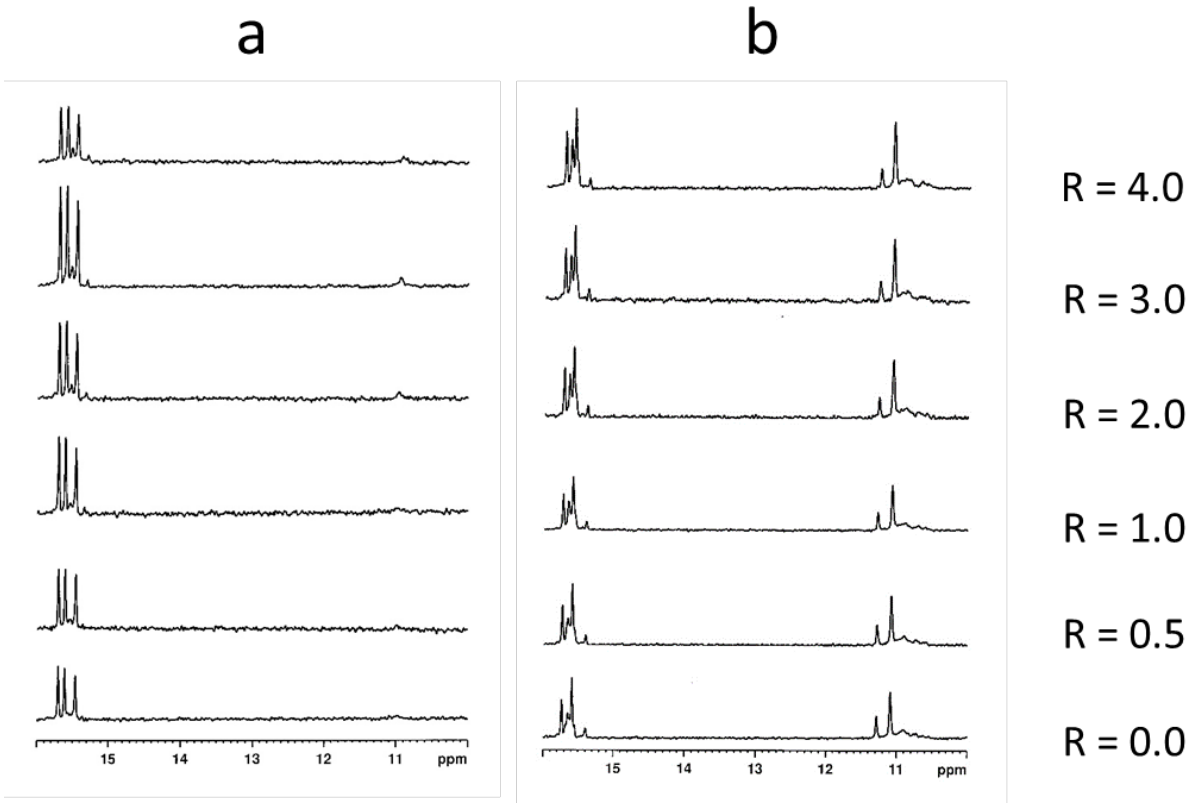

Figure 7.

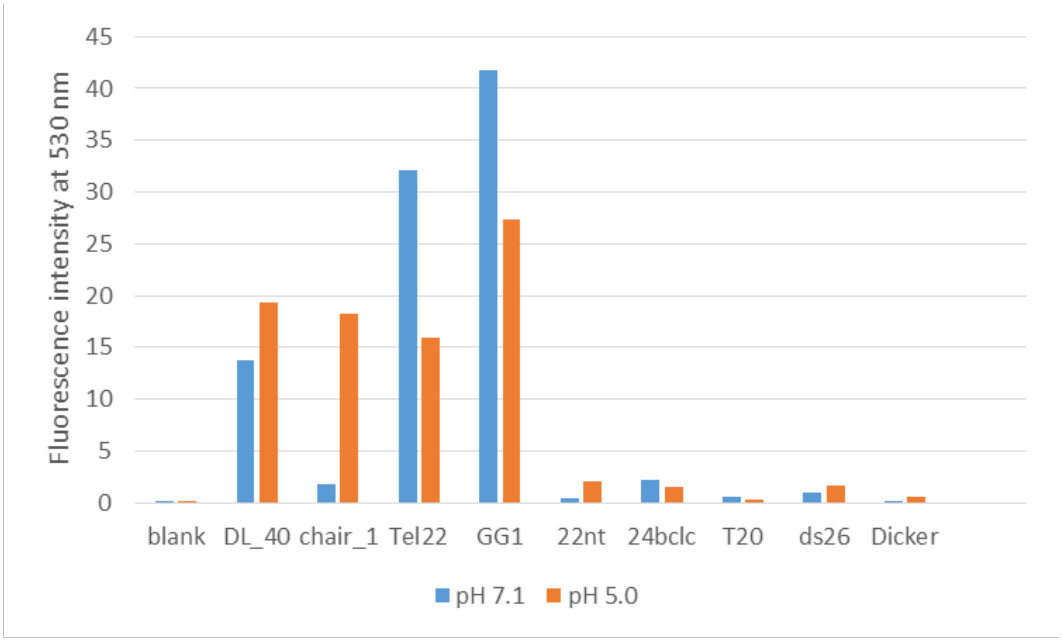
Fluorescence intensity at 530 nm
45
40
35
30
25
20
15
10
5
0
blank
DL_40
chair_1
Tel22
GG1
22nt
24bclc
T20
ds26
Dicker
pH 7.1
pH 5.0

Figure 8.